

# A New Approach to Gene Mutation Analysis Using “GFP-Display”<sup>1</sup>

Takashi Aoki,<sup>2</sup> Rika Ami,<sup>1</sup> Hitoshi Onagi,<sup>1</sup> Hiroyoshi Fujino,<sup>1,†</sup> and Hiroyuki Watabe<sup>1</sup>

<sup>1</sup>Department of Biochemistry, Faculty of Pharmaceutical Sciences, Health Sciences University of Hokkaido, 1757 Kanazawa, Ishikari-Tobetsu, Hokkaido 061-0293; and <sup>2</sup>Katayama Chemical Industries Co., 3-26-22 Higashi-Nanba, Amagasaki 660-0892

Received November 8, 1999; accepted January 26, 2000

The unique behavior of green fluorescent protein (GFP) on SDS-PAGE was applied to the detection of a single amino acid substitution in GFP-tagged polypeptides. This simple detection method using SDS/urea gels was designated GFP-display. The N-terminal 18 or 37 amino acids of K-Ras was used as a model GFP-tagged polypeptide. K-ras exon 1 was fused to a *gfp* cDNA at each end and expressed in *Escherichia coli*. Amino acid number 12 of K-Ras (wild type; Gly) was changed to Ser, Arg, Cys, Asp, Ala, or Val, and the mobility shift of the greenish fluorescent bands in the SDS/urea gel was analyzed. These mutants were easily detected by GFP-display; however, detection depended strongly on the urea concentration and electrophoresis temperature. Subsequently, GFP-display was applied to the 36 amino acids encoding human *p53* exon 7. Amino acid number 248 (wild type; Arg) was changed to Gly, Trp, Gln, Pro, or Leu, and similar mobility shifts were observed. GFP-display could be coupled with an *in vitro* translation system. Fluorescent active GFP and GFP-Ras fusion proteins were synthesized within a few hours. GFP-display shows potential as a modern approach to gene mutation analysis at the protein level, and is a useful method for protein engineering studies.

**Key words:** green fluorescent protein (GFP), GFP-display, K-ras, mutation analysis, *p53*.

SDS-PAGE is one of the most basic and important techniques used in biological and biochemical studies. Here we present a useful SDS-PAGE technique for gene mutation analysis using green fluorescent protein (GFP). GFP from *Aequorea victoria* is now widely used in cell biology as a marker for gene expression and a fusion tag for studying protein localization and secretion systems in living cells (1, 2). GFP is also a useful tool employed in *in vitro* studies. In previous reports on GFP-tagged proteins, we demonstrated that a fluorescence active GFP migrated to a different position from the inactive GFP in SDS-PAGE (3, 4). This mobility shift is thought to be the result of a tight, compact barrel-like structure that possesses unusual resistance to denaturation by SDS (5, 6). In this study we applied this property to the electrophoretic detection of K-ras codon 12 and *p53* codon 248 mutants.

K-ras is a very useful genetic marker employed in the study of several cancers (7–9). Codon 12 of K-ras is known to be a unique hot spot for mutation, and several sensitive detection systems targeting this position have been developed (10–13). Codon 248 of *p53* is also a known hot spot. However, in the case of *p53*, the mutation points are not limited and are found in many codons (14, 15). Therefore,

the detection of *p53* mutation is relatively complicated and difficult to perform. A point mutation in a gene of interest is usually detected by DNA level analysis coupled with PCR, e.g., single strand conformational polymorphism (SSCP) (16), denaturing gradient gel electrophoresis (DGGE) (17), or cleaved fragments length polymorphism (CFLP) (18), and, of course, direct sequencing. However, a gene mutation is not directly linked to the mutation of a gene product. Our objective was to develop a new and simple method to detect a point mutation at the protein level. Only the protein truncation test (PTT) (19) is used for protein level analysis; however, this method measures the molecular mass change of a gene product resulting from a nonsense mutation. GFP-display, described in this report, detects one amino acid change resulting from a missense mutation.

## MATERIALS AND METHODS

**Plasmid Construction**—*Aequorea gfp* cDNA was cloned into pKK223-3 (Amersham Pharmacia Biotech, Uppsala, Sweden), and, to improve the fluorescent activity at high temperatures, serine 147 was changed to proline as described by Kimata *et al.* (20). The resulting plasmid, pGFP147P, was used as a base for all further constructs. Thus, the GFP referred to in the text indicates S147P GFP.

K-ras exon 1 was amplified using standard PCR with the *ras* Mutant Set for c-Ki-ras codon 12 (Takara Shuzo, Tokyo) as the template. A total of seven kinds of fragments were modified using the following primers: 5'-AAAGAATTCAT-GACTGAATATAAACTTGT-3' and 5'-AAACTGCGCTCT-ATTGTTGGATCATATT-3' (*Eco*RI and *Pst*I sites are underlined). After digestion with *Eco*RI and *Pst*I, the fragments

<sup>1</sup> This work was supported in part by a Grant-in-Aid for High Technology Research Program from the Ministry of Education, Sciences, Sports and Culture of Japan.

<sup>2</sup> To whom correspondence should be addressed. Tel: +81-1332-3-1211, Fax: +81-1332-3-1346, E-mail: aokit@hoku-ryo-u.ac.jp

Abbreviations: GFP, green fluorescent protein; SSCP, single strand conformational polymorphism; IPTG, isopropyl- $\beta$ -D-thiogalactopyranoside; CBB, Coomassie Brilliant Blue.

© 2000 by The Japanese Biochemical Society.

were placed on the 5' end of *gfp* cDNA. The resulting plasmids were named pKRAS37(X)G (X = G, S, R, C, D, A, or V). Subsequently, seven kinds of fragments were modified using the following primers: 5'-CCGCGCTGCAGATGACT-GAATATAAACTTGTGGTA-3' and 5'-CGACGAAGCTTTT-ATCACTCTATTGTTGGATCATA-3' (*Pst*I and *Hind*III sites are underlined); and placed at the 3' end of *gfp* cDNA. The resulting plasmids were named pGKRAS37(X).

Human *p53* exon 7 was amplified using following the primers: 5'-AAACTGCAGGTTGGCTCTGACTGTACCAAC-3' and 5'-TTAAGCTTGCATGTAGCTCACTATTAGGAGT-CITCCAGTGTGATGA-3'. One microgram of genomic DNA prepared from human placenta was used as the template. Codon 248 (CGG) was changed to GGG, TGG, CAG, CCG, and CTG by PCR, and these six fragments were placed at the 3' end of *gfp* cDNA. The resulting plasmids were named pGP53EX7(X) (X = R, G, W, Q, P, or L).

Enzymes were purchased from Gibco BRL, Life Technologies (Rockville, MD, USA) or Nippon Gene (Toyama), and all reactions were performed as specified by the manufacturers. Plasmids were transformed into *E. coli* JM109 with  $\text{CaCl}_2$ , and transformants were selected on LB agar plates containing 50  $\mu\text{g}$  ampicillin/ml. Plasmids were purified by the boiling method. The DNA was sequenced using a fluorescence imaging analyzer FMBIO-100 (Takara Shuzo, Tokyo).

**Sample Preparation**—*E. coli* strains harboring each plasmid were grown at 37°C in 10 ml of LB broth until the mid-log phase. After the addition of 0.3 mM (final concentration) isopropyl- $\beta$ -D-thiogalactopyranoside (IPTG; Wako Pure Chemical Industries, Osaka) and further incubation for 10 h at 25°C, the cells were harvested, suspended in 1

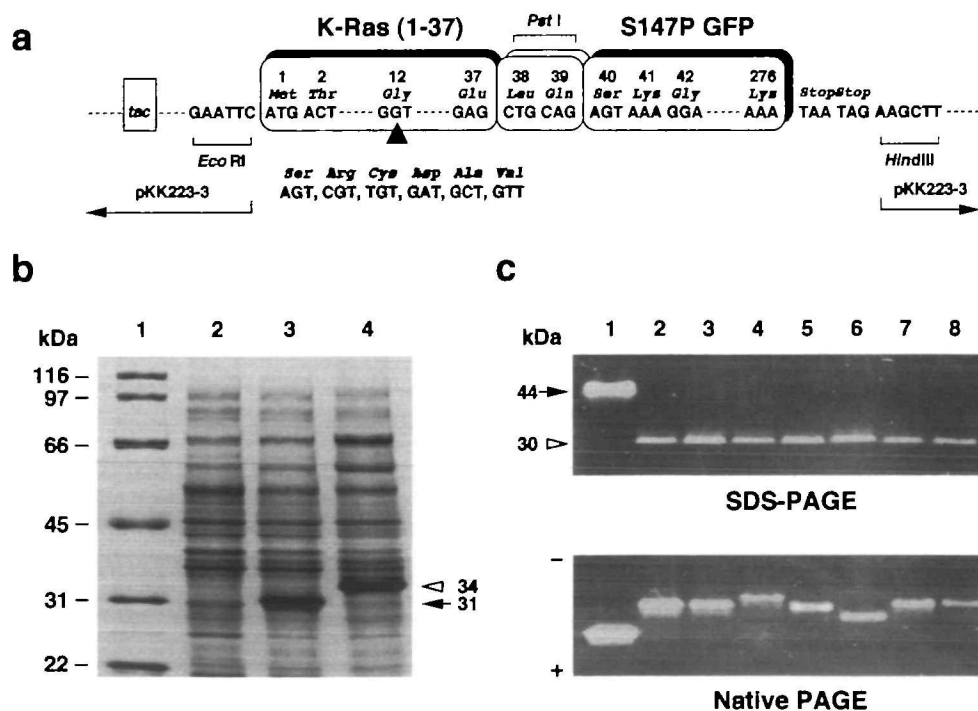
ml of 20 mM Tris-HCl buffer (pH 8.0) containing 30 mM NaCl and 10 mM EDTA, and disrupted by sonic oscillation. The cell extract prepared was used for electrophoretic analysis. *In vitro* translation was performed according to the coupled system (*E. coli* S30 Extract System for Linear Template; Promega, Madison, WI, USA) using 1  $\mu\text{g}$  of plasmid DNA at 30°C.

**Electrophoresis and Detection of GFP**—Proteins were separated in native, SDS, or SDS/urea polyacrylamide gels (7  $\times$  8  $\times$  0.15 cm). Native PAGE was performed in the standard Tris-glycine system using 7.5% gels. SDS-PAGE was performed in 12% gels containing 0.2% SDS at room temperature (20–22°C) or in a chromato-chamber (10°C) according to Laemmli, using a broad range molecular mass standards kit (Bio-Rad Laboratories, Hercules, CA, USA). The separated proteins were stained with 0.25% Coomassie Brilliant Blue (CBB) R-250 and recorded using the gel imaging system "Archiver Eclipse" (Fotodyne Inc., Hartland, WI, USA). The greenish fluorescent bands were detected under UV light (NLMS-20E; UVP, Upland, CA, USA) at 365 nm and recorded on Polapan 3200B (Polaroid, Cambridge, MA, USA) using a green filter.

## RESULTS

**GFP and Ras37(G)-GFP**—The initiation methionine codon of *gfp* cDNA was deleted by PCR and cloned into pKK223-3; subsequently, the DNA fragment encoding the N-terminus with 37 amino acids of wild type K-Ras was amplified and inserted at the 5' end of *gfp* cDNA (Fig. 1a). The resulting plasmid, pKRAS37(G)G, encoded a fusion protein between K-Ras<sup>1–37</sup> (amino acid #12 = Gly) and GFP

**Fig. 1. Construction of pKRAS37(X)Gs and the expression of Ras37(X)-GFPs.** (a) The wild type *ras* fragment encoding the N-terminal 37 amino acids of the six DNA fragments with mutations at codon 12 were placed at the 5' end of *gfp* cDNA (see Table I for details). (b) Cell extracts (5  $\mu\text{l}$ ) prepared from the strain harboring pGFP147P or pKRAS37(G)G were heat-denatured (95°C for 5 min) and resolved in a 0.2% SDS-12% polyacrylamide gel. The loaded samples are as follows: lane 1, molecular mass markers; 2, pKK223-3 (negative control); 3, pGFP147P; 4, pKRAS37(G)G. The gel was stained with CBB. The positions of GFP and Ras37(G)-GFP are indicated by the arrow and arrowhead, respectively. (c) The same samples, 0.5  $\mu\text{l}$  of pGFP147P and 5  $\mu\text{l}$  of pKRAS37(G)G, and other cell extracts (5  $\mu\text{l}$ ) prepared from strains harboring pKRAS37(X)Gs, X = S, R, C, D, A, or V, were resolved without heating in a 12% gel containing 0.2% SDS or a 7.5% native gel. The fluorescent bands were detected by UV light at 365 nm. The bands in each lane are as follows: lane 1, GFP; lanes 2–8, Ras37(X)-GFPs (2, G; 3, S; 4, R; 5, C; 6, D; 7, A; 8, V). The apparent molecular masses of GFP (arrow) and Ras37(G)-GFP (arrowhead) are shown on the left.



[denoted Ras37(G)-GFP] composed of 276 amino acids. GFP or GFP-tagged proteins expressed in *E. coli* often migrate as two individual bands on SDS-PAGE (one fluorescent active, the other inactive) (3, 4, 21). To confirm these phenomena, the cell extracts prepared from *E. coli* strains harboring pGFP147P or pKRAS37(G)G were resolved by SDS-PAGE. GFP produced by pGFP147P was mainly active in the fluorescent form. However, Ras37(G)-GFP produced by pKRAS37(G)G largely formed a non-fluorescent inclusion body. The heat-inactivated GFP and Ras37(G)-GFP migrated to positions corresponding to the originally inactive molecules, and were visible as major bands with molecular masses of 31 and 34 kDa, respectively (Fig. 1b). These molecular masses are almost identical to the theoretical values [27 kDa for GFP and 31 kDa for Ras37(G)-GFP]. Although the fluorescent active GFP and Ras37(G)-GFP were not readily identified as major bands by CBB-staining, they were clearly visible by UV-

irradiation at the 44 and 30 kDa positions, respectively (Fig. 1c). These findings clearly indicate that the active and heat-inactivated molecules differ in mobility on SDS-PAGE as in the case of GFP and Ras37(G)-GFP.

**Ras37(X)-GFPs**—The plasmid set of *K-ras* codon 12 mutants was constructed by replacement of the *ras* fragment of pKRAS37(G)G (Table I). Active Ras37(X)-GFPs (X = G, S, R, C, D, A, or V) were compared by SDS- and native PAGE (Fig. 1c). On SDS-PAGE, Ras37(X)-GFPs migrated to identical positions. However, on native PAGE, the migrating positions depended mainly on their isoelectric points, and Ras37(R)-GFP together with Ras37(D)-GFP bands were different from the wild type.

More notable mobility shifts were observed in SDS gels containing high concentrations of urea (Fig. 2a). Urea reduces the effective pore size of a gel and leads to a decrease in the mobility of proteins (22). All proteins were affected by the addition of urea and their mobilities

TABLE I. Ras-GFP fusion proteins examined by GFP-display

Plasmid	K-ras codon 12	Protein name <sup>a</sup>	M.W. <sup>b</sup>	pI <sup>c</sup>	Hydrophilicity <sup>d</sup>
pGFP147P	—	GFP <sup>e</sup>	26,895	5.64	0.07
pKRAS37(G)G	GGT (wild = Gly)	Ras37(G)-GFP	31,024	5.38 (4.32)	0.04 (-0.19)
pKRAS37(S)G	AGT (Ser)	Ras37(S)-GFP	31,054	5.38 (4.32)	0.04 (-0.19)
pKRAS37(R)G	CGT (Arg)	Ras37(R)-GFP	31,123	5.50 (4.74)	0.05 (-0.11)
pKRAS37(C)G	TGT (Cys)	Ras37(C)-GFP	31,070	5.38 (4.32)	0.04 (-0.22)
pKRAS37(D)G	GAT (Asp)	Ras37(D)-GFP	31,082	5.27 (4.10)	0.05 (-0.11)
pKRAS37(A)G	GCT (Ala)	Ras37(A)-GFP	31,038	5.38 (4.32)	0.04 (-0.21)
pKRAS37(V)G	GTT (Val)	Ras37(V)-GFP	31,066	5.38 (4.32)	0.03 (-0.23)

<sup>a</sup>GFP or Ras-GFP fusion proteins encoded by each plasmid. <sup>b</sup>Molecular weight (M.W.) of each protein was deduced from the corresponding DNA sequence. <sup>c</sup>Isoelectric point (pI) of the Ras segment is shown in parenthesis. <sup>d</sup>Hydrophilicity was calculated according to Hopp and Woods (26), and shown as the average. Hydrophilicity of the Ras segment is indicated in parentheses. <sup>e</sup>GFP used in this study was S147P GFP.

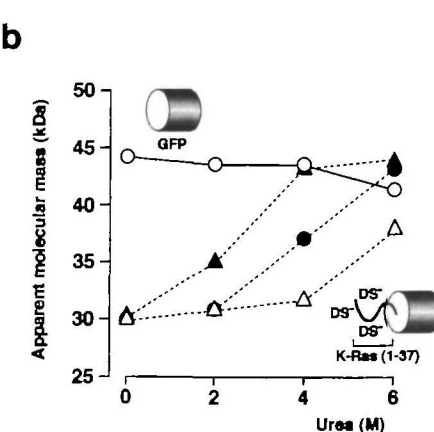
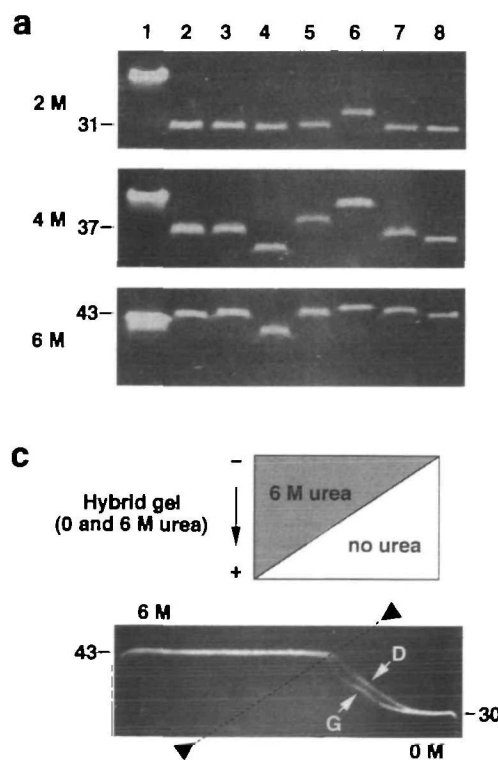
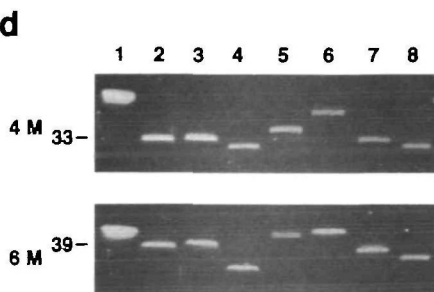
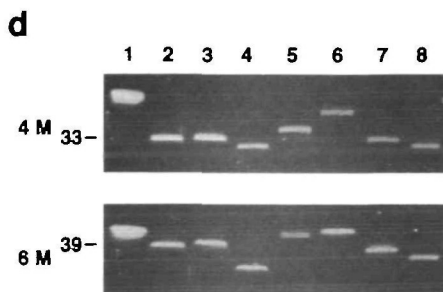


Fig. 2. SDS-PAGE of Ras37(X)-GFPs using urea-containing gels. (a) Cell extracts were resolved at room temperature in 0.2% SDS-12% polyacrylamide gels containing 2, 4, or 6 M urea. Samples are as described for Fig. 1c. The apparent molecular mass of Ras37(G)-GFP is shown on the left in kDa. (b) The apparent molecular masses of GFP (○) and Ras37(X)-GFPs (●, G; △, R; ▲, D) changed with the urea concentration in the gels. Molecular models of GFP and Ras37(X)-GFPs are also illustrated. DS-, dodecyl sulfate ion. (c) A hybrid gel was prepared as shown using 0.2% SDS-12% polyacrylamide gels containing 0 and 6 M urea. Cell extracts (50  $\mu$ l of each) prepared from the strain harboring pKRAS37(G)G or pKRAS37(D)G were mixed and resolved without insertion of the sample combs. The discontinuous line is indicated by arrowheads. The apparent molecular mass is shown on both sides in kDa. G, Ras37(G)-GFP; D, Ras37(D)-GFP. (d) Electrophoresis was performed at 10°C using the same samples.



decreased. However, the behavior of Ras37(X)-GFPs in SDS/urea gels was clearly different from that of GFP. Although the relative position of GFP to the molecular markers was mostly constant (41–44 kDa), the mobility of Ras37(X)-GFPs decreased markedly with increasing urea concentration (Fig. 2, a and b). As shown in Fig. 1c, Ras37(X)-GFPs migrated to the same position on the SDS gel without urea. However, the band positions were notably different with increasing urea concentration (Fig. 2a). The migrating shifts that occurred on 0.2% SDS gels were slightly greater than those on 0.1% SDS gels (data not shown). All fusion proteins, with the exception of Ras37(S)-GFP, migrated to different positions compared to the wild type Ras37(G)-GFP in 4 M urea gels. However, in 6 M urea gels, Ras37(X)-GFPs migrated to almost the same position with the exception of Ras37(R)-GFP. This SDS-PAGE technique using GFP-tagged polypeptides and the urea-containing gel was named GFP-display.

The molecular models of GFP and Ras37(X)-GFPs are shown in Fig. 2b. Ras37(X)-GFPs may move in SDS/urea gels as GFP-labeled "Ras-polypeptides" rather than GFP-fusion proteins. SDS/urea gels allow for the electrophoretic analysis of small polypeptides (22, 23), and it is also commonly known that the electrophoretic mobilities of small polypeptides are strongly influenced by their tertiary structures, which are altered by urea and SDS (24, 25). The tertiary structural change in the "Ras-polypeptides" in SDS/urea gels may be one of the reasons for their remarkable mobility shift. As seen in Fig. 2b, two types of Ras37(X)-GFPs, for example G and D, can be separated as "duplication lines" on a horizontal urea gradient gel (left side, 0 M; right side, 6 M). However, these species were also separated on a more simple hybrid gel composed of 0 and 6 M urea (Fig. 2c). These "duplication lines" probably develop due to the structural changes of the "Ras-polypeptide" with decreasing urea concentration (from 6 to 0 M). The migration positions of Ras37(X)-GFPs were affected not only by urea but also by the electrophoresis temperature (Fig. 2d). This result also suggests that the tertiary structural change of "Ras-polypeptide" influences electrophoretic mobility.

**GFP-Ras18(X)s, GFP-Ras37(X)s, and GFP-p53ex7(X)s** — The *ras* fragments were then inserted at the 3' end of *gfp* cDNA (Fig. 3). The resulting plasmids, pGKRAS37(X)s, encode GFP-Ras37(X)-GFPs composed of 277 amino

acids. The electrophoretic characteristics of the GFP-Ras37(X)s are mainly identical to those of Ras37(X)-GFPs, while GFP-Ras37(X)s requires a higher urea concentration for a shift on the gels to be apparent (Fig. 4). This result

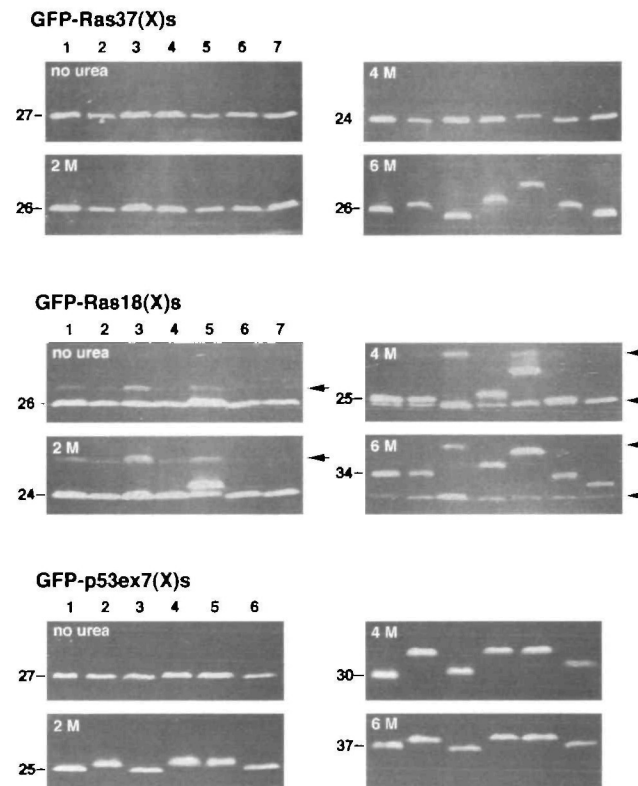


**Fig. 4. Expression of GFP-Ras37(X)s, GFP-Ras18(X)s, and GFP-p53ex7(X)s.** Cell extracts (5  $\mu$ l) prepared from strains harboring pGKRAS37(X)s, pGKRAS18(X)s, or pGP53EX7(X)s were resolved in SDS/urea gels at room temperature. The bands in lanes 1–7 of GFP-Ras37(X)s and GFP-Ras18(X)s are as follows: 1, G; 2, S; 3, R; 4, C; 5, D; 6, A; and 7, V. The bands in lanes 1–6 of GFP-p53ex7(X)s are as follows: 1, R; 2, G; 3, W; 4, Q; 5, P; and 6, L. The apparent molecular masses of GFP-Ras37(G), GFP-Ras18(G), and GFP-p53ex7(R) are shown on the left in kDa. The "urea supersensitive" and "urea resistant" derivatives are indicated by arrows and arrowheads, respectively.

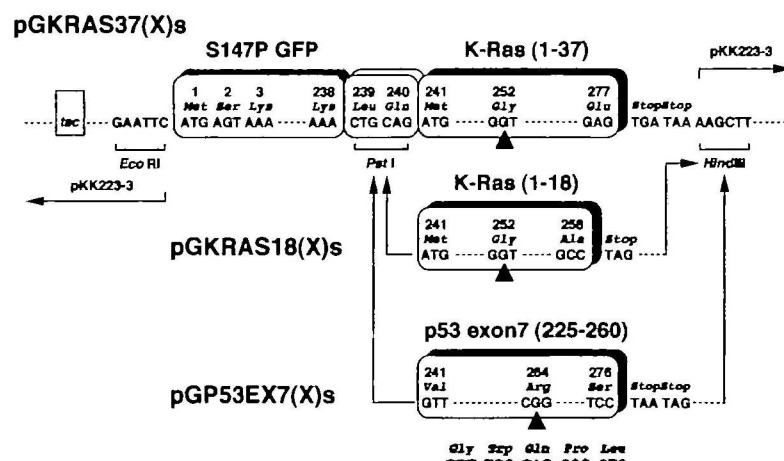


**Fig. 3. Construction of pGKRAS37(X)s, pGKRAS18(X)s, and pGP53EX7(X)s.** The *ras* fragment set encoding the N-terminal 37 or 18 amino acids was placed at the 3' end of *gfp* cDNA. The fragment set of human *p53* codon 248 mutants was placed at the same position. The mutation points are indicated by arrowheads.

suggests that the tertiary structures of the "Ras-polypeptide" at the C terminal are slightly more resistant to changes in urea concentration. To investigate the influence of the polypeptide length on the GFP-display, codon 19 (TTG) of the *ras* fragment was changed to a stop codon (TAG) and inserted at the *Pst*I-*Hind*III site (Fig. 3). Although the band patterns of GFP-Ras18(X)s were basically identical to those of GFP-Ras37(X)s, the mobility shift of each band was more dynamic. In addition, although the reason(s) remains unclear, "urea supersensitive" and "urea resistant" derivatives were also observed (Fig. 4).

The plasmid set of human *p53* codon 248 mutants was constructed by replacement of the *ras* fragment of pGKRAS37(G). The resulting plasmids, pGP53EX7(X)s (X = R, G, W, Q, P, or L), encoded GFP-p53<sup>225-260</sup> fusion pro-

teins [denoted GFP-p53ex7(X)s] composed of 276 amino acids (Fig. 3). The mutation point (*p53* codon 248) corresponded to amino acid #264 of GFP-p53ex7(X)s. All mutants migrated to different positions compared with wild type GFP-p53ex7(R) in 4 M urea gels. However, in 6 M urea gels, all GFP-p53ex7(X)s migrated to position near that of Ras37(X)-GFPs (Fig. 4).

GFP-display was coupled with the *in vitro* translation technique. Active GFP was synthesized in a microtube and clearly visible as a greenish fluorescent band in SDS-PAGE (Fig. 5a). The GFP-Ras18(G) band was considerably weaker than GFP, although somewhat stronger than Ras37(G)-GFP or GFP-Ras37(G). The band positions of GFP and GFP-Ras18(G, D, and R) were identical to those prepared from *E. coli* cells on 0 or 6 M urea gels (Fig. 5b), indicating

**Fig. 5. GFP-display coupled with *in vitro* translation technique.** (a) GFP (lanes 1 and 2), Ras37(G)-GFP (3 and 4), GFP-Ras37(G) (5 and 6), and GFP-Ras18(G) (7 and 8) were synthesized in microtubes and resolved at room temperature in a 0.2% SDS-12% polyacrylamide gel containing no urea. *In vitro* translations were performed on a 25  $\mu$ l scale at 30°C for 3 h (lanes 1, 3, 5, and 7) or 6 h (2, 4, 6, and 8). Ten microliters of each reaction mixture was precipitated with acetone and loaded onto the gel. The apparent molecular masses of GFP and GFP-Ras18(G) are shown on the left in kDa. (b) GFP (lanes 1 and 2), GFP-Ras18(G) (3 and 4), GFP-Ras18(R) (5 and 6), and GFP-Ras18(D) (7 and 8) obtained from living cells (1, 3, 5, and 7) or by *in vitro* translation (2, 4, 6, and 8) were compared on gels containing 0 or 6 M urea. *In vitro* reactions were performed in a 25  $\mu$ l volume at 30°C for 3 h, and all reaction mixtures were subsequently precipitated by acetone and loaded onto gels. (c) Outline of the GFP-display coupled with *in vitro* translation.

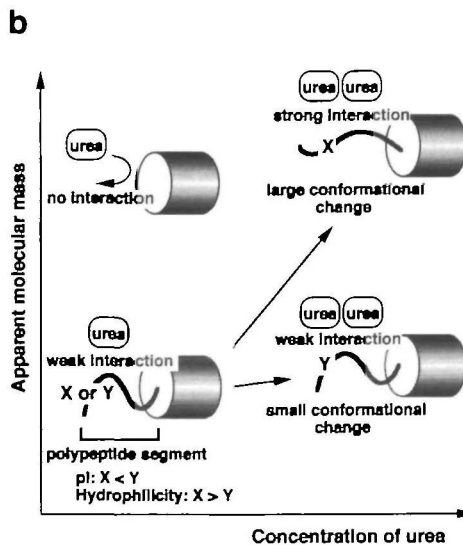
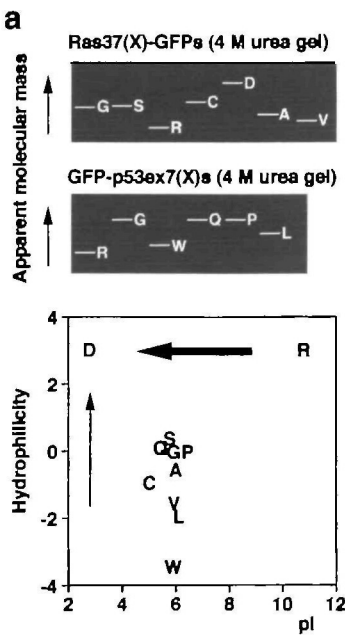
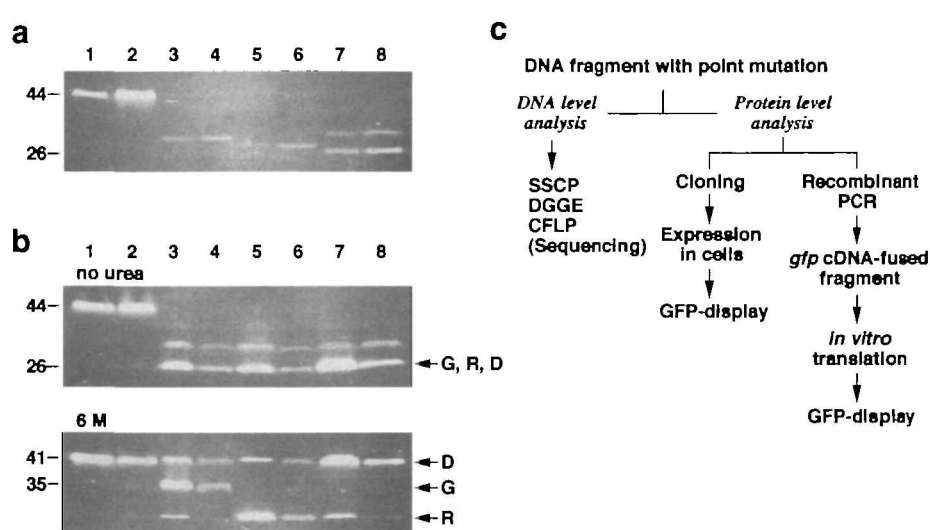


**Fig. 6. A working hypothesis of GFP-display.** (a) The upper two panels indicate the typical patterns of GFP-display in this study. The lower panel is the hydrophilicity and isoelectric point of each amino acid corresponding to the mutation points. The direction and thickness of arrows in the lower panel show the tendency of increasing apparent molecular mass. (b) The migration position of the GFP-tagged polypeptide is influenced by the hydrophilicity and isoelectric point of the polypeptide segment in the SDS/urea gel. See text for details.

that it is also possible to investigate the *in vitro* translated samples using GFP-display. As shown in Fig. 5c, the combination of recombinant PCR and *in vitro* translation is a viable alternative GFP-display. The combination of SSCP and GFP-display may also be a powerful option.

## DISCUSSION

In this report, we present a new SDS-PAGE technique using a GFP-tag. This method, named GFP-display, detects single amino acid changes in polypeptides tagged with GFP. GFP-display is based upon the following unique behaviors of fluorescent active GFP on SDS-PAGE: (i) active GFP and inactive GFP migrate to different positions, and the GFP-tagged polypeptides also possess this property; (ii) the apparent molecular mass of active GFP-tagged polypeptide is lower than that of intact GFP; and (iii) the position of active GFP-tagged polypeptide migration varies on urea-containing gels with one amino acid changes in the polypeptide segment.

An interesting mobility shift on SDS-PAGE corresponding to (i) and (ii) above has been already reported for intact GFP (21) and GFP-tagged proteins (3, 4). It is clear that these unique properties are caused by the compact and tight barrel-like structure, named "β-can," of GFP (6). This structure may give GFP unusual resistance to denaturing reagents or proteases. We consider (i) and (ii) as follows: the β-can structure of active GFP is not destroyed by SDS when unheated; SDS, which can absorb active GFP, is diminished, resulting in slow mobility; the active GFP-tagged polypeptide moves forward from the intact GFP molecule due to the negative charge of the dodecyl sulfate ions absorbed on the polypeptide segment (Fig. 2b).

The reason(s) for (iii) is difficult to understand. From Fig. 2, c and d, although the migration shift may be caused by tertiary structural changes in the polypeptide segment, the apparent mechanism remains unclear. However, as shown in Fig. 6a, it is likely that there is some relationship between the migration positions and amino acid changes. In the upper two panels, the band positions of Ras37(X)-GFPs and GFP-p53ex7(X)s are illustrated. The apparent molecular masses of Ras37(X)-GFPs and GFP-p53ex7(X)s are D>C>G=S>A>V>R and G=Q=P>L>W>R, respectively. The lower panel is the hydrophilicity index (26), and the isoelectric point of each amino acid corresponding to the mutation points. These results suggest that the migration positions are controlled by at least these two factors and that the change in the isoelectric point is more important for the position shift. The apparent molecular mass tends to increase with low isoelectric point and high hydrophilicity of the polypeptide segment. Therefore, GFP-display may efficiently detect an amino acid change which leads to the large change in these factors. From these results, although further studies are required, we consider (iii) as follows: the active GFP region functions as an unchanged "anchor" on the urea-containing gel; therefore, a GFP-tagged polypeptide behaves like a chemically labeled polypeptide on a gel; the strong interaction between urea and the polypeptide segment causes a change in its tertiary structure and decreased mobility; this interaction increases with urea concentration, especially in segments with a higher hydrophilicity and lower isoelectric point (Fig. 6b). However, under conditions of even higher urea concentration (6–8

M), the tertiary structure of any polypeptide may be similar and all may migrate to identical positions.

Of course, the most useful feature of GFP is the fluorescent activity. GFP-display harnesses this powerful advantage in two ways. (a) First, is the easy detection and high sensitivity of fluorescence. GFP-tagged polypeptides were mainly expressed in *E. coli* as fluorescence inactive inclusion bodies. These originally inactive molecules are detected by CBB-staining as major bands on SDS-PAGE with migration positions identical to heat-inactivated molecules. On the other hand, the active molecules are relatively minor components and it is difficult to identify their positions by CBB-staining. However, we could monitor the migration position specifically with ease using only a UV transilluminator. Since the limit of detection of active GFP bands is almost 15 ng (data not shown), it is possible to perform GFP-display using a smaller culture, for example less than 1 ml, or an *in vitro* translation system. (b) The other advantage is the very stable "β-can" structure of the fluorescent active GFP molecule. GFP-display is applicable only to active GFP-tagged polypeptides. Because the active GFP regions with unusual resistance to the denaturing reagents function as an "anchor," and we can analyze structural changes in only the polypeptide segment. If the "anchor" structure is destroyed by SDS or urea, it is impossible to use this method.

GFP-display provides a potentially modern approach to gene mutation analysis at the protein level. However, at present, several problems remain to be resolved. First, we do not have sufficient data concerning the applicable polypeptide length. As the polypeptide length increases, the gap caused by a single amino acid change may decrease. However, this may be influenced not only by the kind and position of the amino acid changed, but also by the concentration of acrylamide or urea in the gel. Secondly, as shown in Fig. 2, a and d, intact GFP appears as two bands in gels containing high concentrations of urea. If some GFP molecules are degraded by proteases at the N- or C-terminal, they ought to be detected on a gel containing no urea. However, only GFP migrating as a single band was detected (Fig. 1c). Moreover, this phenomenon was not observed for GFP-tagged polypeptides. The intact GFP may be expressed in *E. coli* as two (or more) types of molecules with slightly different forms at their terminal ends. Thirdly, in case of GFP-Ras18(X)s, "urea supersensitive" and "urea resistant" derivatives were observed. This suggests that GFP-Ras18(X)s form different tertiary structures, and their responses to urea differ. Currently, we have no concrete data to explain this observation. Since these variants were not detected among GFP-Ras15(X)s, which are made by substituting the *ras* codon 16 for a stop codon (data not shown), the shorter polypeptide length may not be a convincing reason for this phenomenon. This aspect requires further clarification. In this paper, we present the procedure and a working hypothesis for GFP-display. We hope that amino acid substitutions in many kinds of polypeptides will be investigated by GFP-display and the various results will accumulate through the efforts of many researchers. These results will clarify the advantages and disadvantages of GFP-display and confirm our speculations and bring to light unknown problems.

K-ras and p53 mutations are closely related to many kinds of cancers and various critical mutation points have

been revealed. If DNA level analysis such as SSCP is supplemented by GFP-display, more precise analysis is possible. In this study we used well known mutants (the codon 12 of *K-ras* and 248 of *p53*) as typical models. However, this method, may be suitable for the screening of new or position unknown mutations. In conclusion, while several problems remain to be resolved, GFP-display can be used as a simple and useful method for gene mutation analysis and protein engineering studies; for instance, for the screening for site non-specific mutagenic experiments. The detection of mutations depends strongly on the urea concentration and electrophoresis temperature. However, the reproducibility is high, and under suitable conditions, many mutations can be detected by basic and simple electrophoresis.

## REFERENCES

1. Cubitt, A.B., Heim, R., Adams, S.R., Boyd, A.E., Gross, L.A., and Tsien, R.Y. (1995) Understanding, improving and using green fluorescent proteins. *Trends Biochem. Sci.* **20**, 448-455
2. Misteli, T. and Spector, D.L. (1997) Applications of the green fluorescent protein in cell biology and biotechnology. *Nat. Biotechnol.* **15**, 961-964
3. Aoki, T., Takahashi, Y., Koch, K.S., Leffert, H.L., and Watabe, H. (1996) Construction of a fusion protein between protein A and green fluorescent protein and its application to western blotting. *FEBS Lett.* **384**, 193-197
4. Aoki, T., Kaneta, M., Onagi, H., Takahashi, Y., Koch, K.S., Leffert, H.L., and Watabe, H. (1997) A simple and rapid immunoassay system using green fluorescent protein tag. *J. Immunoassay* **18**, 321-333
5. Ormö, M., Cubitt, A.B., Kallio, K., Gross, L.A., Tsien, R.Y., and Remington, S.J. (1996) Crystal structure of the *Aequorea victoria* green fluorescent protein. *Science* **273**, 1392-1395
6. Yang, F., Moss, L.G., and Phillips, G.N., Jr. (1996) The molecular structure of green fluorescent protein. *Nat. Biotechnol.* **14**, 1246-1251
7. Bos, J.L., Fearon, E.R., Hamilton, S.R., Verlaan-de Vries, M., van Boom, J.H., van der Eb, A.J., and Vogelstein, B. (1987) Prevalence of *ras* gene mutations in human colorectal cancers. *Nature* **327**, 293-297
8. Forrester, K., Almoguera, C., Han, K., Grizzle, W.E., and Perucho, M. (1987) Detection of high incidence of *K-ras* oncogenes during human colon tumorigenesis. *Nature* **327**, 298-303
9. Rodenhuis, S., van de Wetering, M.L., Mooi, W.J., Evers, S.G., van Zandwijk, N., and Bos, J.L. (1987) Mutational activation of the *K-ras* oncogene. A possible pathogenetic factor in adenocarcinoma of the lung. *New Engl. J. Med.* **317**, 929-935
10. Ehlen, T. and Dubeau, L. (1989) Detection of *ras* point mutations by polymerase chain reaction using mutation-specific, inosine-containing oligonucleotide primers. *Biochem. Biophys. Res. Commun.* **160**, 441-447
11. Kahn, S.M., Jiang, W., Culbertson, T.A., Weinstein, I.B., Williams, G.M., Tomita, N., and Ronai, Z. (1991) Rapid and sensitive nonradioactive detection of mutant *K-ras* genes via 'enriched' PCR amplification. *Oncogene* **6**, 1079-1083
12. Takeda, S., Ichii, S., and Nakamura, Y. (1993) Detection of *K-ras* mutation in sputum by mutant-allele-specific amplification (MASA). *Hum. Mutat.* **2**, 112-117
13. Fox, J.C., England, J., White, P., Ellison, G., Callaghan, K., Charlesworth, N.R., Hehir, J., McCarthy, T.L., Smith-Ravin, J., Talbot, I.C., Snary, D., Northover, J.M., Newton, C.R., and Little, S. (1998) The detection of *K-ras* mutations in colorectal cancer using the amplification-refractory mutation system. *Br. J. Cancer* **77**, 1267-1274
14. Hollstein, M., Sidransky, D., Vogelstein, B., and Harris, C.C. (1991) *p53* mutations in human cancers. *Science* **253**, 49-53
15. Levine, A.J., Momand, J., and Finlay, C.A. (1991) The *p53* tumour suppressor gene. *Nature* **351**, 453-456
16. Orita, M., Iwahana, H., Kanazawa, H., Hayashi, K., and Sekiya, T. (1989) Detection of polymorphisms of human DNA by gel electrophoresis as single-strand conformation polymorphisms. *Proc. Natl. Acad. Sci. USA* **86**, 2766-2770
17. Myers, R.M., Lumelsky, N., Lerman, L.S., and Maniatis, T. (1985) Detection of single base substitutions in total genomic DNA. *Nature* **313**, 495-498
18. Maddox, L.O., Li, P., Bennett, A., Descartes, M., and Thompson, J.N. (1997) Comparison of SSCP analysis and CFLP analysis for mutation detection in the human iduronate 2-sulfatase gene. *Biochem. Mol. Biol. Int.* **43**, 1163-1171
19. Roest, P.A., Roberts, R.G., Sugino, S., van Ommen, G.J., and den Dunnen, J.T. (1993) Protein truncation test (PTT) for rapid detection of translation-terminating mutations. *Hum. Mol. Genet.* **2**, 1719-1721
20. Kimata, Y., Iwaki, M., Lim, C.R., and Kohno, K. (1997) A novel mutation which enhances the fluorescence of green fluorescent protein at high temperatures. *Biochem. Biophys. Res. Commun.* **232**, 69-73
21. Inouye, S. and Tsuji, F.I. (1994) Evidence for redox forms of the *Aequorea* green fluorescent protein. *FEBS Lett.* **351**, 211-214
22. Swank, R.T. and Munkres, K.D. (1971) Molecular weight analysis of oligopeptides by electrophoresis in polyacrylamide gel with sodium dodecyl sulfate. *Anal. Biochem.* **39**, 462-477
23. Anderson, B.L., Berry, R.W., and Telser, A. (1983) A sodium dodecyl sulfate-polyacrylamide gel electrophoresis system that separates peptides and proteins in the molecular weight range of 2500 to 90,000. *Anal. Biochem.* **132**, 365-375
24. Wiltschi, J., Arold, N., and Neuhoff, V. (1991) A new multiphasic buffer system for sodium dodecyl sulfate-polyacrylamide gel electrophoresis of proteins and peptides with molecular masses 100,000-1000, and their detection with picomolar sensitivity. *Electrophoresis* **12**, 352-366
25. Klagsbli, H.-W., Wiltschi, J., and Staufenbiel, M. (1996) Electrophoretic separation of  $\beta$ A4 peptides (1-40) and (1-42). *Anal. Biochem.* **237**, 24-29
26. Hopp, T.P. and Woods, K.R. (1981) Prediction of protein antigenic determinants from amino acid sequences. *Proc. Natl. Acad. Sci. USA* **78**, 3824-3828